

Article

Assessment of Nutrient Leaching in Flooded Paddy Rice Field Experiment Using Hydrus-1D

Abdikani Abdullahi Mo'allim ¹, Md Rowshon Kamal ^{1,*}, Hadi Hamaaziz Muhammed ¹, Mohd Amin Mohd Soom ², Mohamed Azwan b. Mohamed Zawawi ¹, Aimrun Wayayok ¹ and Hasfalina bt. Che Man ¹

¹ Department of Agricultural Engineering, Faculty of Engineering, Universiti Putra Malaysia, Serdang 43400, Selangor, Malaysia; abdikani51@gmail.com (A.A.M.); hadiazizm@gmail.com (H.H.M.); Mohdazwan@upm.edu.my (M.A.b.M.Z.); aimrun@yahoo.com (A.W.); hasfalina@upm.edu.my (H.b.C.M.)

² Faculty of Sustainable Agriculture, Universiti Malaysia Sabah (UMS), Jalan UMS, Kota Kinabalu 88400, Sabah, Malaysia; mohd.amin@usm.edu.my

* Correspondence: rowshon@yahoo.com; Tel.: +603-89464339

Received: 26 March 2018; Accepted: 11 May 2018; Published: 14 June 2018



Abstract: Solute runoff and leaching are two direct pathways of nutrient pollution from paddy fields into water systems. Due to the dynamic nature of paddy fields, solute transport and transformation processes are complex and difficult to understand. Therefore, in this study, nitrogen (N) transport in flooded paddy rice fields with conventional irrigation (flooding irrigation) in the Tanjung Karang Rice Irrigation Scheme (TAKRIS), Sawah Sempadan, were observed and modelled using the Hydrus-1D numerical model during two consecutive rice growing seasons. Based on solute transport analysis results, it was observed that 50.3% to 48% of percolated N was accumulated in the top 40-cm soil layer, while 49.7% to 52% of leachate N was lost below the 40-cm soil layer (40–100 cm) during the off and main seasons, respectively. About 85% of N leaching loss was in the form of NO_3^- . NO_3^- was absorbed by rice roots within 0–40 cm and the denitrified root zone; however, there was still a large quantity of NO_3^- which remained below the root zone, which was quickly transported downward along with the leachate water. The NH_4^+ concentration in subsurface water was lower than the NO_3^- concentration due to various processes that removed NH_4^+ from the topsoil layer (0–40 cm), such as ammonium volatilisation, nitrification, and plant uptake. The total leaching loss of N was 34.9 and 27.9 kg/ha during the off and main seasons, respectively. The simulated and observed water flow and nutrient leaching were in a good agreement ($R^2 = 0.98$, RMSE = 0.24). The results showed that Hydrus-1D successfully simulated the solute movement under different soil depths during the study period.

Keywords: solute transport; Hydrus-1D; leaching losses; TAKRIS

1. Introduction

The nutrient concentration of surface and subsurface waters has changed into a dangerous worldwide environmental and ecological problem [1], which has tremendously accelerated the potential risks of the eutrophication of surface water and toxic contamination of groundwater. Most chemical fertiliser loads primarily originate from agricultural fields, especially during the rice growing seasons, in which a tremendous amount of fertilisers are utilised within agricultural crops. Urea is the one of the most commonly utilised N fertilisers in rice production systems [2]. However, it is essential to use an ideal quantity of N for optimum handling of rice production in arid and semiarid regions, considering that the implementation of a surplus amount of water can cause nitrogen draining under the root zone and results in economic loss for farmers.

Fertilisers are usually applied in Malaysia by conventional means. In paddy fields, the applied fertilisers, after dissolution, are not only transported over and infiltrate the soil, but are also diffused out and channelled in all possible directions due to the transverse variation of water velocity and depth [3]. Deterioration of water quality in streams and lakes continues to be a significant issue in many counties [4]. Causative factors include not only pollutants from various point sources, but also those from nonpoint sources. The understanding of nutrient/fertiliser transformation in paddy fields is limited due to complex interactions between the soil, water, and biomass [5,6], and the behaviour related to plant growth in paddy soils has been extensively studied [7]. Therefore, forecasting hydrological pathways and pollutants' (nutrient and pesticides) behaviour in paddy soil appears to be crucial to define specific management practices controlling nonpoint source pollution and preserving water resources [8]. Additionally, due to the dynamic nature of paddy rice fields, N transport and transformation processes are complex and difficult to understand. Therefore, the modelling of nutrient dynamics in paddy fields becomes challenging as rice is a highly water- and N-demanding crop.

Several mathematical models are available to describe the water balance and behaviours of nutrients and pesticides in flooded rice fields. Some models describing the fate of nitrogen in rice fields focus on various processes that occur in floodwater, which include PADDY (Pesticide Paddy Field Model) [9], PCPF-1 (Pesticide Concentration in Paddy Field, v.1) [10], RICEWQ (Rice Water Quality) [11,12], and PADDIMOD [13], while others describe mass transport in flood water and the soil underneath. Chung et al. [14] developed the GLEAMS-PADDY model to describe nutrient loading in surface water and groundwater bodies. Chowdary et al. [15] developed and applied a simple model for assessing the concentration of nitrates in water percolating out of the flooded rice fields. Tournebize et al. [8] developed a coupled model (PCPF-SWMS) for simulating the fate and behaviour of pollutants in water and soil of paddy fields. In the GLEAMS-PADDY model [14], the N balance is separated into the $\text{NH}_4\text{-N}$ and $\text{NO}_3\text{-N}$ balances and applied to ponding water and underlying soil. PADDIMOD [13] describes the N balance as the total inorganic N, without focusing on the $\text{NH}_4\text{-N}$ and $\text{NO}_3\text{-N}$ balances separately.

The Hydrus-1D [16] numerical model is one of those that have been widely tested by many researchers to predict nutrient leaching in paddy fields under different irrigation and management practices [17–21]. Li et al. [22] used HYDRUS-1D to estimate the nitrogen transport in the paddy field. They reported that HYDRUS-1D can simulate N transformation in paddy fields and could be a potential tool for optimal fertiliser management practices. Furthermore, Tan et al. [23] used the HYDRUS-1D model to evaluate solute transport in paddy fields under different irrigation practices. They concluded that the HYDRUS-1D model can be an alternative system approach to enhance water and solute management for sustainable rice production. Dash et al. [24] used a HYDRUS-1D model to predict water and nitrate leaching from paddy fields under different fertilisation managements. Based on their simulated results, it was found that there was a good agreement between the HYDRUS-1D model simulation and field data.

However, no work yet has been carried out checking the accuracy of this model for simulating solute transport and leaching in flooded paddy rice fields in the Tanjung Karang rice irrigation scheme (TAKRIS). The scheme practices two cropping seasons to produce two crops of rice per annum, namely the "main season" (July to October) and the "off season" (January to April), which are also referred to as the "wet season" and the "dry season", respectively. The main season crop is harvested in the month of October, whereas the irrigated off season crop is in the months of April and May. During these two seasons, farmers use substantial amounts of N to obtain high yields. However, all N applied is not taken up by rice plants as some of it may percolate below the root zone, which substantially contaminates the quality of groundwater. After applying fertilisers to the field, they dissolve, are transported over the land surface, and infiltrate the soil through irrigation water. In flooded paddy rice fields, the solute may be transported vertically with irrigation water; thus, the HYDRUS-1D model can appropriately demonstrate the distribution of fertilisers through the soil by one-dimensional flow [25]. The objective of this study is to model N leaching in flooded paddy rice

fields at TAKRIS using the Hydrus-1D numerical model. Moreover, in the present study, the suitability of this model for simulating N leaching in paddy fields under flooding irrigation was evaluated.

2. Materials and Methods

2.1. Site Description

The study region relates to the Tanjung Karang rice irrigation scheme, which is located at 3°25'~3°45' N latitude and 100°58'~101°15' E longitude in the state of Selangor, Malaysia. It is one of the several irrigation compartments in Sawah Sempadan, consisting of 1468 lots, with the total area of about 2300 hectares divided into 24 blocks. BLOCK C in the Sawah Sempadan compartment had 86 individual farmers and was chosen as a research study area of the present study as shown in Figure 1. The only source for irrigation supply in Sawah Sempadan is the Berman River. Geographically, the study area is located at 3°28'09.63465" N 101°13'26.48399" E, with average altitude of 6.2 m above the mean sea level. The experimental plot has the soil texture of clay loam, while the texture of the soil surface ranges from clay loam to clay. The soil is classified as Jawa series and defined as clayey, mixed isohyperthermic sulfic tropaquept [26]. The physical and chemical properties of the soil at the site are listed in Tables 1 and 2, respectively.

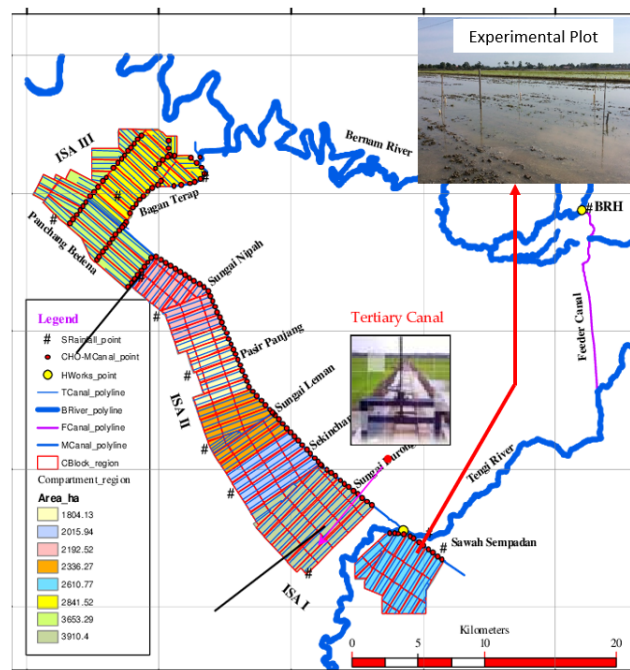


Figure 1. Location of the experimental plot at the Tanjung Karang rice irrigation scheme (TAKRIS), Malaysia.

Table 1. Physical properties of the paddy soil in the experimental field.

| Depth (cm) | Textural Class | Bulk Density (g cm ⁻³) | Saturated Hydraulic Conductivity K _s (cm d ⁻¹) |
|------------|----------------|------------------------------------|---|
| 0–20 | Clay loam | 1.28 | 8.31 |
| 20–40 | Clay loam | 1.33 | 7.58 |
| 40–60 | Clay loam | 1.38 | 7.22 |
| 60–80 | Clay | 1.44 | 6.98 |
| 80–100 | Clay | 1.42 | 6.54 |

Table 2. Chemical properties of the paddy soil in the experimental field.

| Depth (cm) | pH | EC (ms/cm) | Organic Carbon (g kg ⁻¹) | Total Nitrogen (%) | Extractable P (ug/g) | Extractable K (ug/g) |
|------------|------|------------|--------------------------------------|--------------------|----------------------|----------------------|
| 0–20 | 5.44 | 0.40 | 3.7 | 0.27 | 13.72 | 93.7 |
| 20–40 | 5.58 | 0.50 | 3.9 | 0.24 | 12.18 | 201 |
| 40–60 | 5.58 | 0.80 | 2.6 | 0.17 | 11.95 | 215 |
| 60–80 | 5.50 | 0.70 | 2.5 | 0.17 | 11.56 | 211 |
| 80–100 | 5.50 | 0.50 | 2.4 | 0.16 | 11.17 | 222 |

Note: EC = electrical conductivity of the soil.

Experimental Design and Measurements

The study was conducted during two consecutive rice growing seasons (January–April 2017 and July–October 2017) in the Sawah Sempadan irrigation compartment at IADA Selangor. The experimental plot is 0.5 ha (5000 m²) in size. “BLOCK C” was chosen as the study area. After the land preparation, the seeds were evenly broadcasted by hand on the soil during the off and main seasons, respectively. After seeding, the field was irrigated until presaturation. The harvest dates were on April and October for the off and main seasons, respectively. Table 3 illustrates agricultural activities during both seasons. The total growing periods during these two seasons were 100 and 105 days, respectively. Soil samples were collected from the experimental plot to estimate the physical and chemical properties of the soil. Textural analyses were performed using a pipet method [27]. The bulk density was determined using core methods [28]. Saturated hydraulic conductivity was determined using the constant head method [29]. Soil organic carbon was estimated using Walkley and Black’s method [30]. Soil EC was measured by conductivity meter. Total nitrogen and extractable P and K were determined using the CHN-S method.

Table 3. Agricultural activities in the experimental field during two rice growing seasons.

| Seasons | Date | Agricultural Activities |
|-------------|-------------|---|
| Off season | 15 Jan 2017 | Rice broadcasting |
| | 29 Jan 2017 | First fertiliser application; urea 40 kg/ha |
| | 12 Feb 2017 | Second fertiliser application; 17.5:15.5:10 NPK = 80 kg/ha |
| | 11 Mar 2017 | Third fertiliser application; 17:3:25:2 mgo, NPK + 2 mgo = 70 kg/ha |
| | 13 Apr 2017 | Field dried (drainage period) |
| | 17 Apr 2017 | Harvesting |
| Main season | 15 Jul 2017 | Rice broadcasting |
| | 25 Jul 2017 | First fertiliser application; urea 40 kg/ha |
| | 01 Aug 2017 | Second fertiliser application; 17.5:15.5:10 NPK = 80 kg/ha |
| | 16 Aug 2017 | Third fertiliser application; 17:3:25:2 mgo, NPK + 2 mgo = 70 kg/ha |
| | 14 Oct 2017 | Field dried (drainage period) |
| | 17 Oct 2017 | Harvesting |

Note: N = Nitrogen; P = Phosphorous; K = Potassium and mgo = magnesium oxide.

Ceramic porous cups at the depths of 20 cm, 40 cm, 60 cm, 80 cm, and 100 cm were installed at five different places to collect the amount of leachate water (solutes) to the subsurface as shown in Figure 2. The percolation rate was calculated by the difference between the bottom closed and opened lysimeters (Figure 3). In Sawah Sempadan, conventional flooding practice is generally adopted in rice paddy fields; therefore, during the entire experimental period, the irrigation and drainage of the experimental plot were monitored. Five porous pipes with leachate collectors were installed to obtain water samples from the subsurface soil in a paddy field. A one-litre plastic bottle was used to collect the samples of subsurface water. Leachate samples were collected on a weekly basis with vacuum hand pump. Additionally, leachate water samples were collected three times within the first 10 days of the fertiliser application. In this period (since the fertiliser application date), the concentration of nutrients varies very significantly. Finally, the samples were transported in a cooler with ice to the

water quality laboratory lab, Faculty of Engineering, UPM, for further analysis. The concentrations of nitrate nitrogen ($\text{NO}_3\text{-N}$) and ammonia nitrogen ($\text{NH}_4\text{-N}$) in these water samples were analysed using a Spectrophotometer DR/890 colorimeter. The amounts of $\text{NO}_3\text{-N}$ and $\text{NH}_4\text{-N}$ loss by leaching during the rice growing season were determined by multiplying the total amount of water leachate measured weekly, and the concentration of these nutrients of water was collected in ceramic porous cups at 20 cm, 40 cm, 60 cm, 80 cm, and 100 cm, respectively.

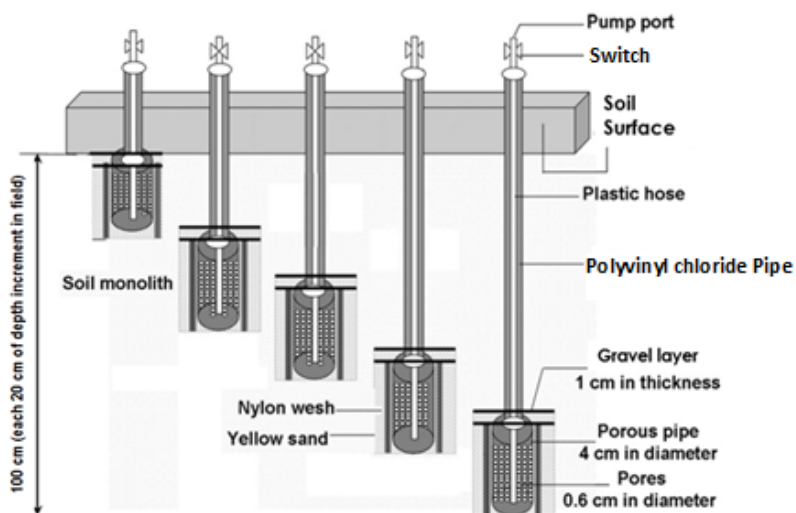


Figure 2. Porous cup soil water samplers installed at 20 cm, 40 cm, 60 cm, 80 cm, and 100 cm in a paddy field.



Figure 3. Monitoring daily percolation rate using field lysimeters in the experimental plot.

In the experimental field, a Parshall RBC flume, drainage sensor, rain gauge, and water level recorder were installed as shown in Figure 4. The amount of precipitation was measured using a data-logging rain gauge. During both seasons, the total amount of rainfall was 47 and 21 cm, respectively. The highest rainfall occurred in the month of January during the off season (23 January 2017), which was 8.7 cm day^{-1} . This area experiences a humid equatorial climate with bimodal rainfall patterns largely influenced by the southwest and northeast monsoons. Rainfall is strongly seasonal, with roughly 70% occurring between the months of October and January during the northeast monsoon, while dry months generally fall in February to March and June to August during the southwest monsoon period. However, rainfall distribution is unreliable from January to August; therefore, the crop has to rely to a large extent on irrigation for sustained yields [31,32].

There was very little variation in the day length and temperature in the area. High temperatures are experienced during the dry season, with mean temperature values ranging from 28 °C to 35 °C. Fairly high humidity is experienced, with an average of 77%, which is typical of tropical climates. The amounts of irrigation water and the flow rate were measured using a Parshall RBC flume with an MJK 7070 level sensor with a CR200X logger (SZ-CR200X/7070) whenever an irrigation event occurred. The total amount of irrigation supply was 69.4 and 68.9 cm for both seasons, respectively. During the experimental period, the field water level was maintained from 3 cm to 10 cm depth until one week before harvesting time and every drainage event. The water level was measured using an E-water level sensor. In addition, the irrigation water was reapplied to maintain the crop water requirement when there was no rainfall (dry period) and the water level fell below a maintained depth.

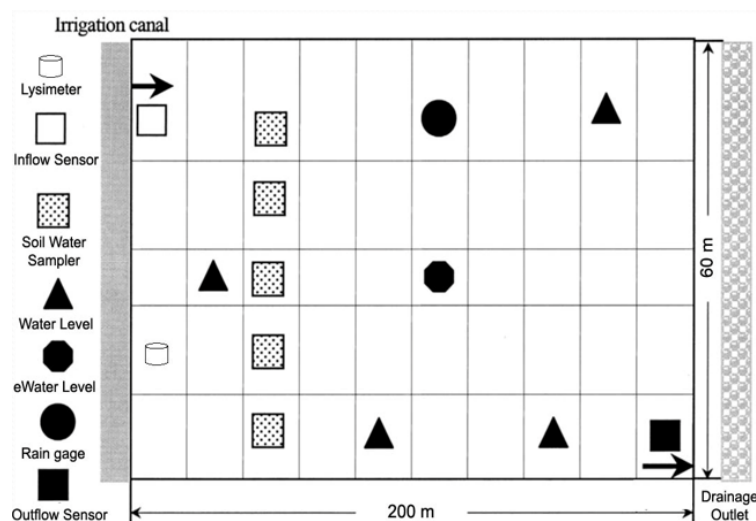


Figure 4. Layout of the equipment installation for the field investigation of water balance components in a paddy field.

An MJK7060 level sensor (NB-CR200X/7060) was installed at the outlet point to measure the amount of drainage water whenever a runoff event occurs. A concrete sump (70 cm × 50 cm × 70 cm) was constructed inside the outlet point to install the level sensor (NB-CR200X/7060). The drainage data was downloaded on a weekly basis during the study period. The total amount of drainage was 43 and 39 cm for both seasons, respectively. Percolation rate was estimated using four lysimeters. Two open and two closed field lysimeters were installed to estimate deep percolation. In the open condition, the lysimeter gives percolation (P) plus evapotranspiration ET (P + ET), while the closed lysimeter estimates only ET. The percolation rate can be obtained from the subtraction. Finally, the average readings from the four lysimeters (Closed, Opened, and Closed and Opened) were recorded as the daily deep percolation rate. The total amount of percolation water was 19.9 cm for the off season and 17.3 cm for the main season, respectively.

After obtaining the N concentrations by laboratory tests, the solute losses from subsurface/leachate were calculated as follow [33]:

$$\text{Subsurface losses (kg ha}^{-1}\text{)} = 0.01 \times C \times DP \quad (1)$$

where C = solute concentration (mg/L) and DP = deep percolation depth (mm).

2.2. Hydrus-1D Model

The HYDRUS-1D model described by Simunek et al. [16] was selected to simulate water flow and solute transport in the experimental field. The governing flow and transport equations were

numerically solved using a Galerkin-type linear finite element scheme. It has been widely used in applications ranging from water flow to solute and heat transfer in vadose zones.

2.2.1. Model Parameters

Hydrus-1D requires four main sets of processes: Soil hydraulic parameters, solute parameters, solute reaction parameters, and root water uptake.

2.2.2. Estimation of Soil Hydraulic Parameters

The van Genuchten soil hydraulic parameters [34] θ_r , θ_s , k_s , m , α , and l , which are required by the model, were estimated using the ROSSETA [35] software package provided by Hydrus-1D regarding soil texture. The pore connectivity (l) was assumed to be equal to 0.5 for many soils [16].

2.2.3. Nitrogen Transport and Transformations

The partial differential equations governing one-dimensional advective–dispersive N transport in variably saturated paddy soils were taken as [22]:

Urea (Total Nitrogen, TN):

$$\frac{\partial \theta c_1}{\partial t} = \frac{\partial}{\partial z} \left(\theta D_1^w \frac{\partial c_1}{\partial z} \right) - \frac{\partial q c_1}{\partial z} - u'_{w,1} \theta c_1 \quad (2)$$

Ammonium nitrate (NH_4^+ -N):

$$\begin{aligned} \frac{\partial \theta c_2}{\partial t} + \frac{\partial \rho s_2}{\partial t} + \frac{\partial a v g_2}{\partial t} = & \frac{\partial}{\partial z} \left(\theta D_2^w \frac{\partial c_2}{\partial z} \right) + \frac{\partial}{\partial z} \left(a v D_2^g \frac{\partial g_2}{\partial z} \right) - \frac{\partial q c_2}{\partial z} - u'_{w,2} \theta c_2 + u'_{w,1} \theta c_1 \\ & + \gamma s_{,2} \rho - r a_{,2} \end{aligned} \quad (3)$$

Nitrate (NO_3^- -N):

$$\frac{\partial \theta c_3}{\partial t} = \frac{\partial}{\partial z} \left(\theta D_3^w \frac{\partial c_3}{\partial z} \right) - \frac{\partial q c_3}{\partial z} - u_{w,3} \theta c_3 + u'_{w,2} \theta c_2 - r a_{,3} \quad (4)$$

where C = solute concentration in the liquid phase (mg L^{-1}); S = solute concentration in the solid phase (mg g^{-1}); g = solute concentration in the gas phase (mg L^{-1}); θ = volumetric water content ($\text{cm}^3 \text{cm}^{-3}$); ρ = dry bulk density (g cm^{-3}); q = volumetric flux density (cm day^{-1}); $u w$ = first-order rate constant for solute in the liquid phase (day^{-1}); $u' w$ is the similar first-order rate constant, providing concentrations between individual chain species; γs is the zero-order rate constant in the solid phase (day^{-1}); $r a$ is the root nutrient uptake ($\text{mg L}^{-1} \text{day}^{-1}$); D_w is the dispersion coefficient for the liquid phase ($\text{cm}^2 \text{day}^{-1}$); and D^g is the diffusion coefficient ($\text{cm}^2 \text{day}^{-1}$) for the gas phase. The subscripts of 1, 2, and 3 represent the N species urea, NH_4^+ -N, and NO_3^- -N, respectively. The adsorption isotherm relating s_2 and c_2 was described using a linear equation of the form:

$$S_2 = k_{d,2} c_2 \quad (5)$$

where $k_{d,2}$ is the distribution coefficient for NH_4^+ -N (L mg^{-1}).

N transformations considered in Equations (2)–(4) were hydrolysis, mineralisation, fixation, volatilisation, nitrification, and denitrification in paddy fields [15,16]. In the present study, hydrolysis, nitrification, and denitrification were all considered as first-order reactions [36], while mineralisation, which is the key N source for rice production [37], was considered as a zero-order process.

2.2.4. Solute Transport and Reaction/Transformation Parameters

For solute transport parameters, molecular diffusion coefficients in free water (D^w) for ammonium and nitrate were 1.5 and 1.64 $\text{cm}^2 \text{day}^{-1}$, respectively [22]; the molecular diffusion coefficient in air

(D^a) for NH_3 was $18,057.6 \text{ cm}^2 \text{ day}^{-1}$; and the longitudinal dispersivity (DL) was equal to 12 cm [38]. It was difficult to measure solute transport and reaction parameters at the laboratory or field scale. Therefore, the values under different soil depths were obtained from published literature and listed in Table 4 [15,22]. Urea hydrolysis was assumed to be equal to 0.74 day^{-1} . According to a previous work [15], mineralisation and immobilisation are the two important solute transformation processes that occur in flooded soils. The constant rate of mineralisation was reported to be 0.0045 day^{-1} [15,22], whereas the constant rate of nitrification from ammonium to nitrate varied between 0.02 and 0.25 day^{-1} . The denitrification rate coefficient varied between 0.01 and 0.06 day^{-1} . The distribution coefficient (K_d) for NH_4^+ -N for different soil layers were taken from a previous work [39]. However, it was assumed that urea and nitrate were only present in the dissolved phase ($K_d = 0 \text{ L mg}^{-1}$) [40].

Table 4. Solutes transported and reaction parameters obtained by model calibration [22].

| Soil Depth (cm) | k_m (day^{-1}) | K_d (L mg^{-1}) | K_n (day^{-1}) | K_{dn} (day^{-1}) | K_h (day^{-1}) |
|-----------------|-----------------------------|------------------------------|-----------------------------|--------------------------------|-----------------------------|
| 0–20 | 0.0045 | 1.8 | 0.25 | 0.05 | 0.74 |
| 20–40 | - | 1.5 | 0.22 | 0.06 | - |
| 40–60 | - | 1.2 | 0.14 | 0.04 | - |
| 60–80 | - | 1.0 | 0.04 | 0.02 | - |
| 80–100 | - | 1.0 | 0.02 | 0.01 | - |

Note: k_m is the comprehensive production rate of NH_4^+ -N that represents mineralisation; K_d is the distribution coefficient for NH_4^+ -N; K_n is the nitrification rate; K_{dn} is the denitrification rate; and K_h is the urea hydrolysis rate.

2.2.5. Initial and Boundary Conditions

For water flow analysis, the initial boundary condition was defined using the observed soil moisture content. The upper boundary condition was defined as the atmospheric boundary condition (BC) by assigning the values of precipitation, evaporation, and irrigation. Due to the saturated condition of the topsoil in the paddy field, a stagnant water depth of 10 cm was considered as the initial condition. The bottom boundary condition was assigned as the free drainage boundary condition since the water table was far below the root zone. For solute transport analysis, the initial concentrations of NO_3^- and NH_4^+ were applied as the initial boundary conditions of solute transport.

2.2.6. Model Evaluation Criteria

Checking the capability of the model to predict the parameters of water flow and solute transport in paddy field requires the evaluation of agreement between the Hydrus-1D-predicted NO_3^- and NH_4^+ values and the observed field data. In this regard, two statistical procedures were used: the coefficient of determination (R^2) and the root mean square error (RMSE), which can be calculated as:

Regression coefficient:

$$R^2 = 1 - \frac{\sum_{i=1}^N (O_i - P_i)^2}{\sum_{i=1}^N (O_i - \bar{O}_i)^2} \quad (6)$$

Root mean square error:

$$\text{RMSE} = \sqrt{\frac{\sum_{i=1}^n (P_i - O_i)^2}{n}} \quad (7)$$

where P is the predicted values, O_i is the observed values, and \bar{O} is the mean of the observed values. The optimum values of R^2 and RMSE are 1 and 0, respectively.

3. Results

3.1. Model Assessment

In the present study, the model was calibrated using the van Genuchten soil hydraulic parameters θ_r , θ_s , m , α , and l , as well as the coefficient of dispersivity of the soils with the measured field

data of the daily concentration of NO_3^- and NH_4^+ at 20, 40, 60, 80, and 100 cm soil depths during the off season. During the calibration period, an inverse estimation was implemented for these soil hydraulic parameters. To decrease the uncertainties of parameter optimisation, the saturated hydraulic conductivity was selected for calibration. In solute transport, calibration and validation processes are very complex and often complicated due to various parameters that need to be examined. Therefore, in this current study, solute transport and reaction parameters that needed to be simultaneously determined were obtained from the literature [22] and listed in Table 4. After a successful calibration, the solute data of NO_3^- and NH_4^+ observed during the main season under different soil depths were utilised to validate the Hydrus-1D model. Table 5 illustrates the optimised values of the soil hydraulic parameters used during the validation period. The accuracy of the model was assessed in calibration and validation stages by statistical parameters. The relationship between simulated and measured data was evaluated using the coefficient of determination (R^2) and the root mean square error (RMSE) as shown in Table 6.

Table 5. Optimised values of soil hydraulic parameters.

| Soil Depth (cm) | Soil Type | θ_r $\text{cm}^3 \text{cm}^{-3}$ | θ_s (cm) | α | n | L | K_s (cm day^{-1}) |
|-----------------|-----------|---|-----------------|----------|--------|-----|--------------------------------|
| 0–20 | Clay loam | 0.0792 | 0.4418 | 0.0158 | 1.4145 | 0.5 | 10.25 |
| 20–40 | Clay loam | 0.0792 | 0.4418 | 0.0158 | 1.4145 | 0.5 | 9.34 |
| 40–60 | Clay loam | 0.0792 | 0.4418 | 0.0158 | 1.4145 | 0.5 | 8.55 |
| 60–80 | Clay | 0.0982 | 0.4588 | 0.0150 | 1.2529 | 0.5 | 8.1 |
| 80–100 | Clay | 0.0982 | 0.4588 | 0.0150 | 1.2529 | 0.5 | 7.2 |

Table 6. Statistical parameters for the evaluation of the model.

| Season | Depth (cm) | Solute Parameters | R^2 | RMSE (mg/L) |
|------------------------------------|------------|-------------------|-------|-------------|
| Off season (calibration period) | 20–40 | NO_3^- | 0.84 | 0.15 |
| | 60–100 | | 0.59 | 0.11 |
| | 20–40 | NH_4^+ | 0.70 | 0.08 |
| | 60–100 | | 0.67 | 0.06 |
| Main season (validation period) | 20–40 | NO_3^- | 0.68 | 0.32 |
| | 60–100 | | 0.59 | 0.23 |
| | 20–40 | NH_4^+ | 0.71 | 0.15 |
| | 60–100 | | 0.69 | 0.10 |

As shown in Table 6, the simulated solute concentrations at different soil depths during the off season were in line with the observed field data. During the calibration period, the model had well predicted the solute concentration at the root zone (0–40 cm), with $R^2 = 0.84$ and $\text{RMSE} = 0.15$ mg/L for NO_3^- and $R^2 = 0.70$ and $\text{RMSE} = 0.08$ mg/L for NH_4^+ . Furthermore, it determined solute concentration below the root zone (60–100 cm) satisfactorily, with $R^2 = 0.60$ and $\text{RMSE} = 0.11$ mg/L for NO_3^- and $R^2 = 0.67$ and $\text{RMSE} = 0.06$ mg/L for NH_4^+ . Similar results were obtained during the main season for the validation period: within the root zone, $R^2 = 0.68$ and $\text{RMSE} = 0.32$ mg/L for NO_3^- , and $R^2 = 0.71$ and $\text{RMSE} = 0.15$ mg/L for NH_4^+ ; below the root zone, $R^2 = 0.59$ and $\text{RMSE} = 0.23$ mg/L for NO_3^- , and $R^2 = 0.69$ and $\text{RMSE} = 0.10$ mg/L for NH_4^+ .

3.2. Dynamic Characteristics of Solutes in Subsurface Water

Figures 5–12 display the comparison between the observed and Hydrus-1D-simulated NO_3^- and NH_4^+ data under the 20, 40, 60, 80, and 100 cm soil depths during two consecutive rice growing seasons, respectively. From the information in Figures 3–10, it was apparent that within the 0–40 cm soil layer, the Hydrus-1D model accurately predicted the NO_3^- movement in the soil for both seasons.

Moreover, the model satisfactorily simulated N movement below the root zone (60–100 cm), but not as well as that simulated within the root zone. The concentration within the root zone was higher compared to below the root zone due to the direct contact of the top surface layer with the chemical fertiliser applied and stagnating water depth.

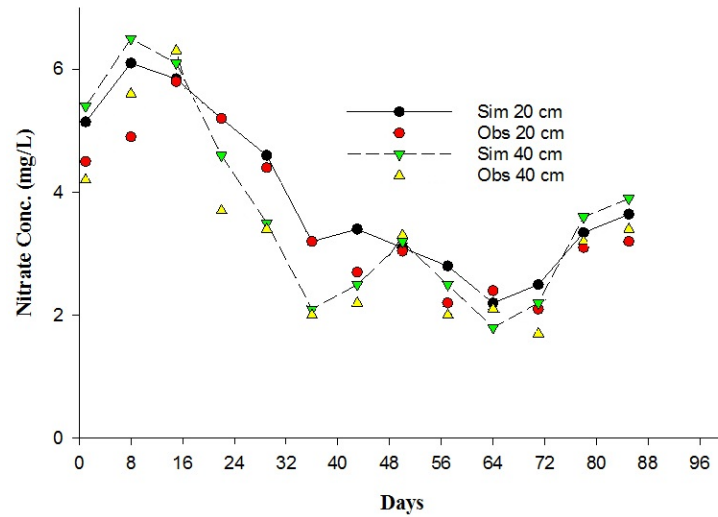


Figure 5. Comparison between simulated (Sim) and observed (Obs) NO₃⁻ concentrations within the root zone (0–40 cm) during the off season.

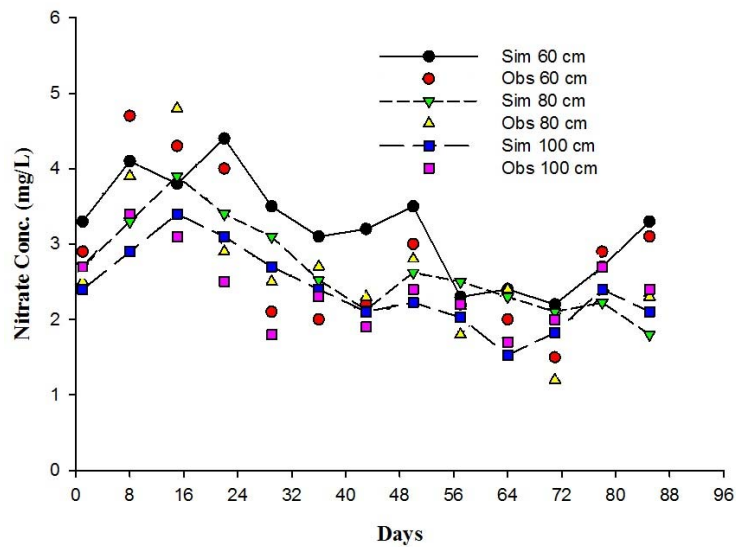


Figure 6. Comparison between simulated and observed NO₃⁻ concentrations below the root zone (60–100 cm) during the off season.

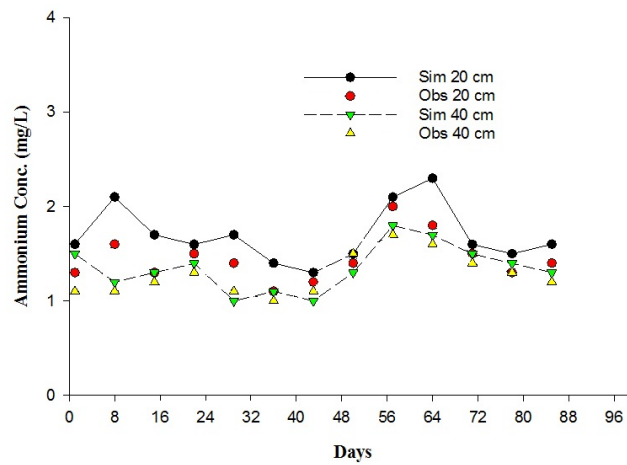


Figure 7. Comparison between simulated and observed NH_4^+ concentrations within the root zone (0–40 cm) during the off season.

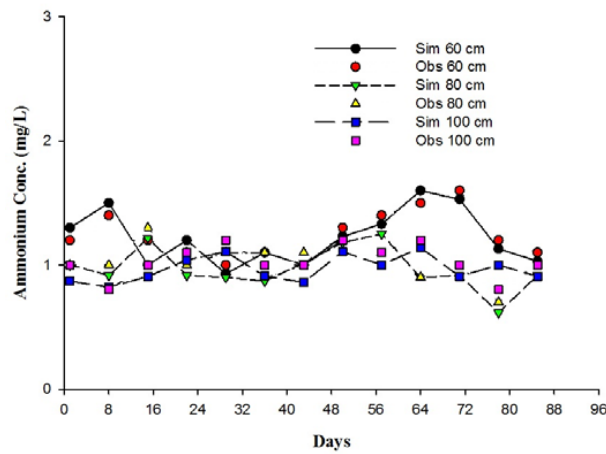


Figure 8. Comparison between simulated and observed NH_4^+ concentrations below the root zone (60–100 cm) during the off season.

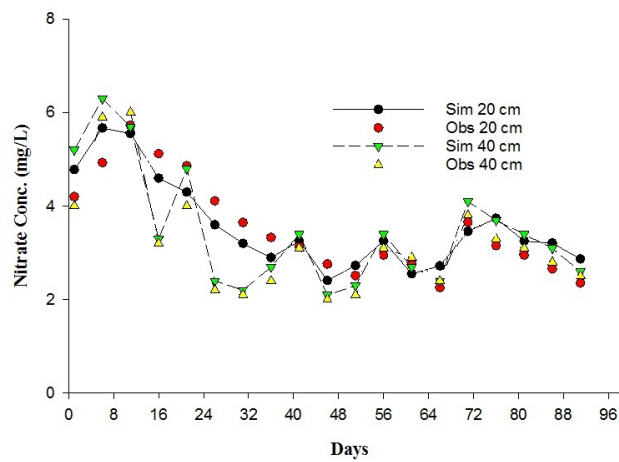


Figure 9. Comparison between simulated and observed NO_3^- concentrations within the root zone (0–40 cm) during the main season.

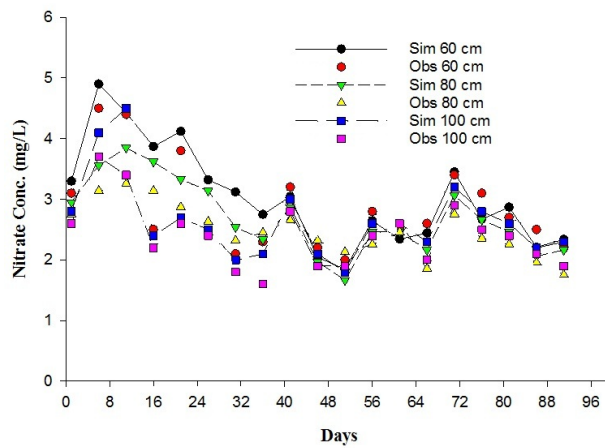


Figure 10. Comparison between simulated and observed NO_3^- concentrations below the root zone (60–100 cm) during the main season.

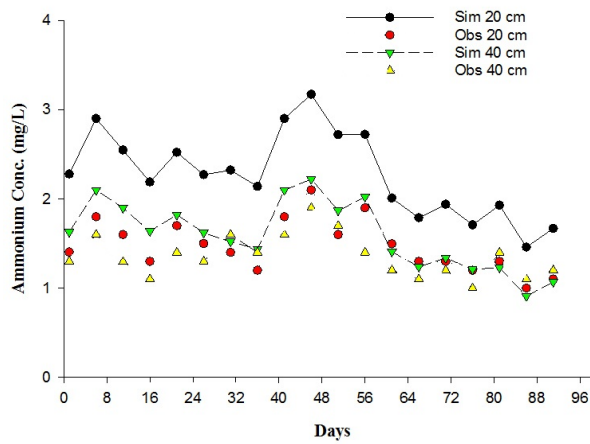


Figure 11. Comparison between simulated and observed NH_4^+ concentrations within the root zone (0–40 cm) during the main season.

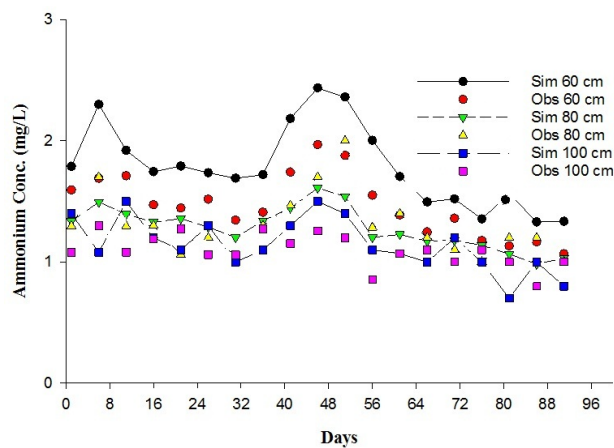


Figure 12. Comparison between simulated and observed NH_4^+ concentrations below the root zone (60–100 cm) during the main season.

Based on the simulated and observed data, the NH_4^+ concentrations within the root zone were slightly higher than those below the root zone. This may be due to nitrification of NH_4^+ to NO_3^- in

subsurface water and plant consumption. The calibrated and validated results suggested that the model results of NH_4^+ at different soil depths mostly matched closely with observed data. Both observed and simulated NH_4^+ showed similar patterns during both seasons. The NH_4^+ within the root zone was lower compared to NO_3^- due to plant uptake. Since rice prefers NH_4^+ to NO_3^- as a source of N [5,40], in the presence of both, rice seeding can take up NH_4^+ faster than NO_3^- [22,41]. Also, nitrification of NH_4^+ to NO_3^- was very fast, explaining the lower concentration of NH_4^+ in the root zone compared to NO_3^- . The nitrate-N concentrations in leachate water ranged from 1.2 to 6.5 mg/L during the rice growing periods. The mean concentrations of $\text{NO}_3\text{-N}$ at five different depths below the surface were 3.6, 3.3, 2.8, 2.7, and 2.4 mg/L, respectively.

The mean concentrations of ammonium-nitrogen in percolation water were 1.4, 1.3, 1.2, 1.0, and 1.0 mg/L at five different depths below the surface, respectively. It ranged from 0.7 to 2.1 mg/L during the experimental period. During both seasons, the concentration of $\text{NO}_3\text{-N}$ increased after the first fertiliser application and then started to decrease gradually. During the off season, the concentration of $\text{NO}_3\text{-N}$ increased from all leachate samples during the rice maturity stage (8–15 April 2017). The concentration of $\text{NO}_3\text{-N}$ in subsurface water at the depth of 20 cm was the highest among leachate water samples collected at different soil depths, which was due to the progress of nitrification under aerobic conditions at the root zone. It was revealed that two weeks before harvest, NO_3^- concentration at the 40-cm topsoil layer had remarkably increased for the off season. However, the declining of the NO_3^- concentration with increasing soil depth reveals that denitrification in the deeper soil layer could be an important pathway of nitrate loss [42]. At the same time, the NO_3^- concentration in leachate water declined during flooding condition periods due to the anaerobic soil environment for denitrification. The concentration of $\text{NH}_4^+\text{-N}$ had slightly increased after the first, second, and third fertiliser applications, respectively. However, the concentration of $\text{NH}_4^+\text{-N}$ in leachate water declined with increasing soil depth.

3.3. Leaching Losses of N in Paddy Fields

Figures 13 and 14 present the Hydrus-1D-simulated cumulative NO_3^- and NH_4^+ fluxes at the bottom of the soil layer (100 cm) during two rice growing seasons. The daily NO_3^- and NH_4^+ fluxes below the root zone were 0.13 and 0.015 kg/ha during the off season and were 0.53 and 0.27 kg/ha during the main season, respectively. The leaching fluxes of NO_3^- were almost the same during both seasons.

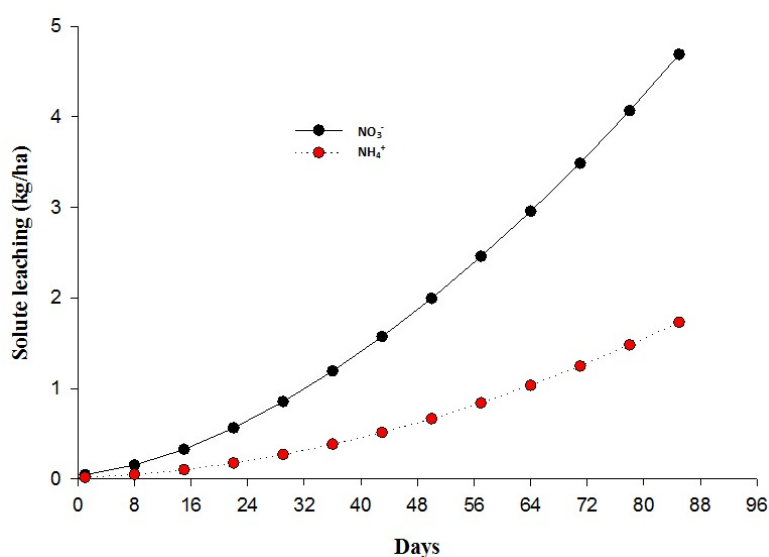


Figure 13. Simulated cumulative leaching fluxes of NO_3^- and NH_4^+ at the bottom of the soil layer (100 cm) during the off season.

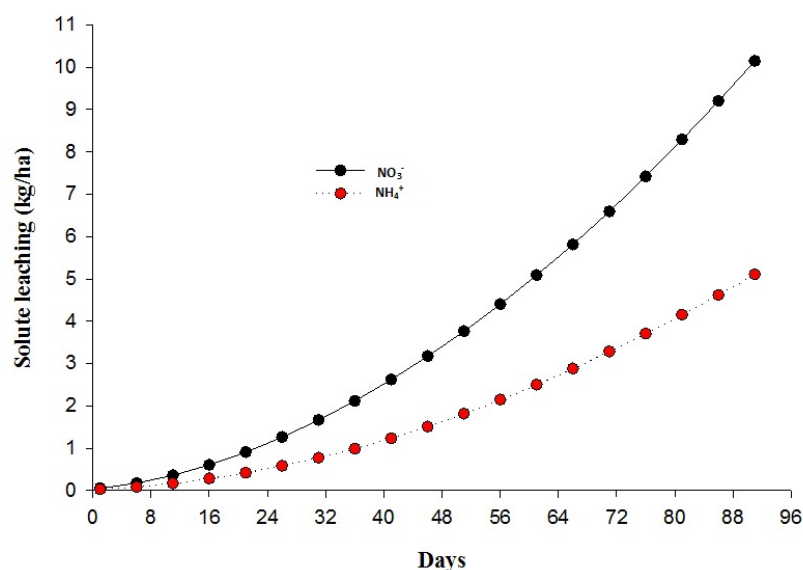


Figure 14. Simulated cumulative leaching fluxes of NO_3^- and NH_4^+ at the bottom of the soil layer (100 cm) during the main season.

The vertical fluxes of N during the two seasons showed a similar trend. The model predicted that the NO_3^- and NH_4^+ fluxes at the bottom 100 cm were 4.7 and 10.1 kg/ha and 1.7 and 5.1 kg/ha for the off and main seasons, respectively. The simulated results of N in the present study was somehow close to those reported previously [43], estimating the total N leaching at the 100-cm soil depth in transplanted paddy rice fields and found to be 5.82 kg/ha during the 2009 rice growing season. In the present study, the overall results of N leaching at the bottom soil were very close to the observed data, which was also similar to previous studies on nutrient leaching losses at the bottom soil layer [39,44]. Furthermore, Dash et al. [24] revealed that the performance of the Hydrus-1D model for simulating N fluxes at the 100-cm soil depth during the two seasons was highly satisfactory.

The total loss of NH_4^+ was less than that of NO_3^- , suggesting that NH_4^+ was easily adsorbed by soil particles and only small amount leached down to the root zone. However, the NH_4^+ loads ranged from 1.9 to 3.9 kg/ha, in which 44.4% to 55.6% of percolated NH_4^+ was accumulated below the 40-cm soil layer. The total vertical flux of NH_4^+ at the 40-cm soil layer was 5.4 kg/ha for the off season and 4.9 kg/ha for the main season, respectively. The reason for this was that there were various processes that removed NH_4^+ from the topsoil layers, such as ammonia volatilisation, N plant uptake, and nitrification in the root zone [45]. During heavy raining periods (off season) from mid-January to the end of February, the N leaching was high due to the flooding water conditions. The ratios of NH_4^+ to NO_3^- were 33.7% during the off season and 38% during the main season, respectively. Additionally, NO_3^- below 40 cm was higher due to the process that elevated the concentration of NO_3^- in the root zone, which was actually a nitrification of NH_4^+ .

4. Discussion

Approximately 45.7% to 46.9% and 53.1 to 55.6% of NO_3^- was accumulated in the top 40 cm and the below-60 cm soil layers during the two seasons, respectively. Since paddy rice is a shallow-rooted crop, it can only absorb and uptake NO_3^- up to the 30–40 cm root zone. However, a large amount of NO_3^- remained below the root zone and was transported downward along with leachate water. The average quantity of NO_3^- ranged from 4.5 to 6.6 kg/ha, while the total vertical flux of NO_3^- was 29.3 kg/ha for the off season and 25.3 kg/ha for the main season, respectively. During the off season, the mean cumulative losses of NO_3^- and NH_4^+ in subsurface water (20–100 cm) were 2.7 and 1 kg/ha, respectively. During the main season, the mean cumulative losses of NO_3^- and NH_4^+ in subsurface water (20–100 cm) were 1.8 and 0.8 kg/ha, respectively. As the paddy plant is shallow-rooted and can

take up nutrients from up to 40 cm, it was thus considered that there were nutrient losses below the root zone, that is, below 40 cm. In this regard, the mean cumulative losses of NO_3^- and NH_4^+ below 40 cm (40–100 cm) during the off season were 2.4 and 0.9 kg/ha, respectively. During the main season, the mean cumulative losses of NO_3^- and NH_4^+ below 40 cm (40–100 cm) were 1.6 and 0.7 kg/ha, respectively. Based on the experimental results, it can be stated that the cumulative losses of NO_3^- and NH_4^+ decreased with increasing soil depth.

The observed total leaching loss of N was 34.9 and 27.9 kg/ha during the off and main seasons, respectively. This resulting tendency was almost similar to a previous study [24], in which the authors estimated N leaching below a 120-cm depth of soil and found a total loss of 28.5 kg/ha. However, it was less than those reported by another group [23], who recorded a total N leaching loss of 13.5 kg/ha during a single rice growing season. This was also higher than that reported elsewhere [46], where it was found that 12.4 kg/ha of N was lost through leachate. Perhaps this difference was mainly due to different fertiliser application, irrigation methods, and types of soil. Furthermore, high N leaching loss could be resulted from the high hydraulic conductivity of the plow pan soil [8]. The ratios of the total amount of N loss via leaching to the applied amount of chemical fertiliser were 22% and 17.6% in the off and main seasons, respectively. Yoon et al. [41] discovered the ratios of N losses through the subsurface of the paddy field to be 9.8%, which was a little higher than those reported previously [39,40]. Almost 55% of N leaching losses occurred during early stages, and more than 80% of nitrogen losses were seen in the form of NO_3^- . Similar results were reported by others [22,41]. In this study, N leaching losses through the subsurface were significant. During the rice cultivation period, the observed N loss of the soil layer below 100 cm was 4.8 kg/ha. This was similar to the result obtained by other authors [43], in which an N leaching loss below 100 cm of 3.46 kg/ha was found.

5. Conclusions

Based on solute transport analysis results, it was observed that about 50.3% to 48% of percolated N was accumulated in the top 40-cm soil layer, while 49.7% to 52% of leachate N was lost below the 40-cm soil layer (40–100 cm) during the off and main seasons, respectively. About 85% of N leaching loss was in the form of NO_3^- . NO_3^- was absorbed by rice roots within the 0–40 cm and denitrificated root zone; however, there was still a large quantity of NO_3^- that remained below the root zone, which was quickly transported downward along with the leachate water. The NH_4^+ concentrations in subsurface water were lower than the N and NO_3^- concentrations due to various processes that removed NH_4^+ from the topsoil layer (0–40 cm), such as ammonium volatilisation, nitrification, and plant uptake.

A comparison between the Hydrus-1D outputs and observed solute data from the paddy field indicates that the model has made sufficiently accurate predictions. In all figures, it was clear that the outputs of the model were mostly very close to the observed field experiment. The results revealed that the model had accurately predicted solute fluxes within the root zone compared to the below root zone results for both seasons. On other hand, the results confirmed that as the soil depth in the experiment increases, the difference between the model-predicted and field-observed data increased. These differences may be due to the results of rapid movement of water under different depths, without sufficient time for reaction between the soil and the solutes [47]. Another important reason was that the time taken by the solutes to reach up to 80–100 cm soil depth may be more than those within the root zone. This was mainly because of the decrease in saturated hydraulic conductivity [44]. Due to the conventional overflooding of the soil in paddy fields during the rice growing period, the soil within the root zone dispersed more as hydraulic conductivity decreased. Previously, researchers [18,22] confirmed that the Hydrus-1D model could be a successful tool for predicting N transport and transformation under both transplanted paddy rice (TPR) and direct seeded rice field (DSR) conditions. In the present study, the overall results revealed that Hydrus-1D simulations were reasonable and effective for simulating the solute transport in flooded paddy rice experimental fields.

Author Contributions: A.A.M. and M.R.K. designed the experiment and wrote the paper, H.H.M. analyzed the data, M.A.M.S., M.A.b.M.Z., A.W. and H.b.C.M. contributed, material and numerical analysis.

Funding: This research was funded by Ministry of Science, Technology and Innovation (MOSTI) grant number “5450774” And Putra-Grant, grant number “9411100”.

Acknowledgments: The authors wish to thank the Ministry of Sciences, Technology and Innovation (MOSTI) and University Putra Malaysia (UPM) for sponsoring this research. This research is funded by the Ministry of Sciences, Technology and Innovation (MOSTI) under e-science grant number escience5450774 and Putra-Grant 9411100.

Conflicts of Interest: The authors declare no conflict of interest.

References

- Chandna, P.; Khurana, M.L.; Ladha, J.K.; Punia, M.; Mehla, R.S.; Gupta, R. Spatial and seasonal distribution of nitrate-N in groundwater beneath the rice–wheat cropping system of India: A geospatial analysis. *Environ. Monit. Assess.* **2011**, *178*, 545–562. [[CrossRef](#)] [[PubMed](#)]
- Ghosh, B.C.; Bhat, R. Environmental hazards of nitrogen loading in wetland rice fields. *Environ. Pollut.* **1998**, *102*, 123–126. [[CrossRef](#)]
- Strelkoff, T.S.; Tamimi, A.H.; Clemmens, A.J. Two-dimensional basin flow with irregular bottom configuration. *J. Irrig. Drain. Eng.* **2003**, *129*, 391–401. [[CrossRef](#)]
- ICID. *Experiences in Inter-Basin Water Transfers for Irrigation, Drainage or Flood Management*; International Commission on Irrigation and Drainage: New Delhi, India, 2005.
- Ishii, S.; Ikeda, S.; Minamisawa, K.; Senoo, K. Nitrogen cycling in rice paddy environments: Past achievements and future challenges. *Microbes Environ.* **2011**, *26*, 282–292. [[CrossRef](#)] [[PubMed](#)]
- Nakasone, H.; Abbas, M.A.; Kuroda, H. Nitrogen transport and transformation in packed soil columns from paddy fields. *Paddy Water Environ.* **2004**, *2*, 115–124. [[CrossRef](#)]
- De Datta, S.K. Improving nitrogen fertilizer efficiency in lowland rice in tropical Asia. *Fertil. Res.* **1986**, *9*, 171–186. [[CrossRef](#)]
- Tournebize, J.; Watanabe, H.; Takagi, K.; Nishimura, T. The development of a coupled model (PCPF-SWMS) to simulate water flow and pollutant transport in Japanese paddy fields. *Paddy Water Environ.* **2006**, *4*, 39–51. [[CrossRef](#)]
- Inao, K.; Kitamura, Y. Pesticide paddy field model (PADDY) for predicting pesticide concentrations in water and soil in paddy fields. *Pestic. Sci.* **1999**, *55*, 38–46. [[CrossRef](#)]
- Watanabe, H. Simulation of Pesticide Concentrations in Paddy Field by PCPF-1 Model-In case of Mefenacet and its control of runoff and leaching. In Proceedings of the XiV Memorial CIGR World Congress, Tsukuba, Japan, 28 November–1 December 2000.
- Williams, M.W.; Ritter, A.M.; Cheplick, M.J.; Zdinak, C.E. RICEWQ: Pesticide runoff model for rice crops. In *User’s Manual and Program Documentation. 1999, Version 1*; Waterborne Environmental, Inc.: Leesburg, VA, USA, 2017.
- Karpouzias, D.G.; Capri, E. Risk analysis of pesticides applied to rice paddies using RICEWQ 1.6. 2v and RIVWQ 2.02. *Paddy Water Environ.* **2006**, *4*, 29–38. [[CrossRef](#)]
- Jeon, J.H.; Yoon, C.G.; Ham, J.H.; Jung, K.W. Model development for surface drainage loading estimates from paddy rice fields. *Paddy Water Environ.* **2005**, *3*, 93–101. [[CrossRef](#)]
- Chung, S.O.; Kim, H.S.; Kim, J.S. Model development for nutrient loading from paddy rice fields. *Agric. Water Manag.* **2003**, *62*, 1–7. [[CrossRef](#)]
- Chowdary, V.M.; Rao, N.H.; Sarma, P.B.S. A coupled soil water and nitrogen balance model for flooded rice fields in India. *Agric. Ecosyst. Environ.* **2004**, *103*, 425–441. [[CrossRef](#)]
- Šimůnek, J.; van Genuchten, M.T.; Šejna, M. Development and applications of the HYDRUS and STANMOD software packages and related codes. *Vadose Zone Journal* **2008**, *7*, 587–600. [[CrossRef](#)]
- Phogat, V.; Yadav, A.K.; Malik, R.S.; Kumar, S.; Cox, J. Simulation of salt and water movement and estimation of water productivity of rice crop irrigated with saline water. *Paddy Water Environ.* **2010**, *8*, 333–346. [[CrossRef](#)]
- Sutanto, S.J.; Wenninger, J.; Coenders-Gerrits, A.M.J.; Uhlenbrook, S. Partitioning of evaporation into transpiration, soil evaporation and interception: A comparison between isotope measurements and a HYDRUS-1D model. *Hydrol. Earth Syst. Sci.* **2012**, *16*, 2605–2616. [[CrossRef](#)]

19. Kandelous, M.M.; Kamai, T.; Vrugt, J.A.; Simunek, J.; Hanson, B.; Hopmans, J.W. Evaluation of subsurface drip irrigation design and management parameters for Alfalfa. *Agric. Water Manag.* **2012**, *109*, 81–93. [[CrossRef](#)]
20. Ramos, T.B.; Šimůnek, J.; Gonçalves, M.C.; Martins, J.C.; Prazeres, A.; Pereira, L.S. Two-dimensional modeling of water and nitrogen fate from sweet sorghum irrigated with fresh and blended saline waters. *Agric. Water Manag.* **2012**, *111*, 87–104. [[CrossRef](#)]
21. Siyal, A.A.; Bristow, K.L.; Šimůnek, J. Minimizing nitrogen leaching from furrow irrigation through novel fertilizer placement and soil surface management strategies. *Agric. Water Manag.* **2012**, *115*, 242–251. [[CrossRef](#)]
22. Li, Y.; Šimůnek, J.; Zhang, Z.; Jing, L.; Ni, L. Evaluation of nitrogen balance in a direct-seeded-rice field experiment using Hydrus-1D. *Agric. Water Manag.* **2015**, *148*, 213–222. [[CrossRef](#)]
23. Tan, X.; Shao, D.; Gu, W.; Liu, H. Field analysis of water and nitrogen fate in lowland paddy fields under different water managements using HYDRUS-1D. *Agric. Water Manag.* **2015**, *150*, 67–80. [[CrossRef](#)]
24. Dash, C.J.; Sarangi, A.; Adhikary, P.P.; Singh, D.K. Simulation of Nitrate Leaching under Maize–Wheat Cropping System in a Semi-arid Irrigated Area of the Indo-Gangetic Plain, India. *J. Irrig. Drain. Eng.* **2015**, *142*, 04015053. [[CrossRef](#)]
25. Tafteh, A.; Sepaskhah, A.R. Application of HYDRUS-1D model for simulating water and nitrate leaching from continuous and alternate furrow irrigated rapeseed and maize fields. *Agric. Water Manag.* **2012**, *113*, 19–29. [[CrossRef](#)]
26. Soil Survey Staff. *Soil Taxonomy: A Basic System of Soil Classification for Making and Interpreting Soil Surveys*; USDA: Washington, DC, USA, 1975.
27. Miller, W.P.; Miller, D.M. A micro-pipette method for soil mechanical analysis. *Commun. Soil Sci. Plant Anal.* **1987**, *18*, 1–5. [[CrossRef](#)]
28. Black, C.A. *Methods of Soil Analysis*; ACSESS: Madison, WI, USA, 1965.
29. Klute, A.; Dirksen, C. Hydraulic conductivity and diffusivity: Laboratory methods. In *Methods of Soil Analysis: Part 1—Physical and Mineralogical Methods*; ACSESS: Madison, WI, USA, 1986; pp. 687–734.
30. Walkley, A.; Black, I.A. An examination of the Degtjareff method for determining soil organic matter and a proposed modification of the chromic acid titration method. *Soil Sci.* **1934**, *37*, 29–38. [[CrossRef](#)]
31. JICA; DID. *The Study on Modernization of Irrigation Water Management System in the Granary Area of Peninsular Malaysia*; Final Report; Japan International Cooperation Agency (JICA): Tokyo, Japan, 1998.
32. Rowshon, M.K.; Amin, M.S.M.; Mojid, M.A.; Yaji, M. Estimated evapotranspiration of rice based on pan evaporation as a surrogate to lysimeter measurement. *Paddy Water Environ.* **2014**, *12*, 35–41. [[CrossRef](#)]
33. Ali, M.H. Pollution of water resources from agricultural fields and its control. In *Practices of Irrigation On-Farm Water Management*; Springer: New York, NY, USA, 2011; Volume 2, pp. 241–269.
34. Van Genuchten, M.T. A closed-form equation for predicting the hydraulic conductivity of unsaturated soils. *Soil Sci. Soc. Am. J.* **1980**, *44*, 892–898. [[CrossRef](#)]
35. Schaap, M.G.; Leij, F.J.; Van Genuchten, M.T. Rosetta: A computer program for estimating soil hydraulic parameters with hierarchical pedotransfer functions. *J. Hydrol.* **2001**, *251*, 163–176. [[CrossRef](#)]
36. Hanson, B.R.; Šimůnek, J.; Hopmans, J.W. Evaluation of urea–ammonium–nitrate fertigation with drip irrigation using numerical modeling. *Agric. Water Manag.* **2006**, *86*, 102–113. [[CrossRef](#)]
37. Gaydon, D.S.; Probert, M.E.; Buresh, R.J.; Meinke, H.; Suriadi, A.; Dobermann, A.; Bouman, B.; Timsina, J. Rice in cropping systems—Modelling transitions between flooded and non-flooded soil environments. *Eur. J. Agron.* **2012**, *39*, 9–24. [[CrossRef](#)]
38. Lotse, E.G.; Jabro, J.D.; Simmons, K.E.; Baker, D.E. Simulation of nitrogen dynamics and leaching from arable soils. *J. Contam. Hydrol.* **1992**, *10*, 183–196. [[CrossRef](#)]
39. Liang, X.Q.; Chen, Y.X.; Li, H.; Tian, G.M.; Ni, W.Z.; He, M.M.; Zhang, Z.J. Modeling transport and fate of nitrogen from urea applied to a near-trench paddy field. *Environ. Pollut.* **2007**, *150*, 313–320. [[CrossRef](#)] [[PubMed](#)]
40. Iqbal, M.T. Nitrogen leaching from paddy field under different fertilization rates. *Malays. J. Soil Sci.* **2011**, *15*, 101–114.
41. Sik Yoon, K.; Kyu Choi, J.; Gwon Son, J.; Young Cho, J. Concentration profile of nitrogen and phosphorus in leachate of a paddy plot during the rice cultivation period in southern Korea. *Commun. Soil Sci. Plant Anal.* **2006**, *37*, 1957–1972. [[CrossRef](#)]

42. Seol, S.I.; Lee, S.M.; Han, G.H.; Choi, W.J.; Yoo, S.H. Urea transformation and nitrogen loss in waterlogged soil column. *Agric. Chem. Biotechnol.* **2000**, *43*, 86–93.
43. Zhao, X.; Zhou, Y.; Min, J.; Wang, S.; Shi, W.; Xing, G. Nitrogen runoff dominates water nitrogen pollution from rice-wheat rotation in the Taihu Lake region of China. *Agric. Ecosyst. Environ.* **2012**, *156*, 1–11. [[CrossRef](#)]
44. Salehi-Lisar, S.Y.; Bakhshayeshan-Agdam, H. Drought Stress in Plants: Causes, Consequences, and Tolerance. In *Drought Stress Tolerance in Plants*; Springer: Cham, Switzerland, 2016; pp. 1–16.
45. Hou, H.; Zhou, S.; Hosomi, M.; Toyota, K.; Yosimura, K.; Mutou, Y.; Nisimura, T.; Takayanagi, M.; Motobayashi, T. Ammonia emissions from anaerobically-digested slurry and chemical fertilizer applied to flooded forage rice. *Water Air Soil Pollut.* **2007**, *183*, 37–48. [[CrossRef](#)]
46. Peng, S.Z.; Yang, S.H.; Xu, J.Z.; Luo, Y.F.; Hou, H.J. Nitrogen and phosphorus leaching losses from paddy fields with different water and nitrogen managements. *Paddy Water Environ.* **2011**, *9*, 333–342. [[CrossRef](#)]
47. Hillel, D. *Environmental Soil Physics: Fundamentals, Applications, and Environmental Considerations*; Elsevier: New York, NY, USA, 1998.



© 2018 by the authors. Licensee MDPI, Basel, Switzerland. This article is an open access article distributed under the terms and conditions of the Creative Commons Attribution (CC BY) license (<http://creativecommons.org/licenses/by/4.0/>).